Chemistry & Biology
Article

A Triazine Compound S06 Inhibits Proinvasive Crosstalk between Carcinoma Cells and Stromal Fibroblasts via Binding to Heat Shock Protein 90

Da-Woon Jung,[1] Jinmi Kim,[1] Zhong Min Che,[2] Eun-Sang Oh,[1] Gicheon Kim,[1] Soo Hyun Eom,[1] Sin-Hyeog Im,[1] Hyung-Ho Ha,[3] Young-Tae Chang,[4,5,6] Darren R. Williams,[1,*] and Jin Kim[2,*]
[1]New Drug Targets Laboratory, School of Life Sciences, Gwangju Institute of Science and Technology, Gwangju 500-712, Republic of Korea
[2]Department of Oral Pathology, Oral Cancer Research Institute, Brain Korea 21 Project, Yonsei University College of Dentistry, Seoul 120-752, Republic of Korea
[3]College of Pharmacy, Sunchon National University, Sunchon 570-742, Republic of Korea
[4]Department of Chemistry
[5]Medicinal Chemistry Program
National University of Singapore, 3 Science Drive 3, Singapore 117543
[6]Laboratory of Bioimaging Probe Development, Singapore Bioimaging Consortium, Agency for Science, Technology and Research (A*STAR), Singapore 138667
*Correspondence: jink@yuhs.ac (J.K.), darren@gist.ac.kr (D.R.W.)
DOI 10.1016/j.chembiol.2011.10.001

SUMMARY

Carcinoma-associated fibroblasts (CAFs) promote tumor invasion by secreting soluble factors. A tagged triazine library was screened in our novel transwell coculture model of CAF and oral squamous cell carcinoma (OSCC). We discovered compound S06, which reduced OSCC invasion by inhibiting secretion of CAF-derived proinvasive chemokines. The N-terminus of Hsp90 was found to be the cellular target of S06. Importantly, S06 did not induce hepatic toxicity, a side effect associated with well-known Hsp90 inhibitors. Moreover, S06 inhibited tumor cell migration in a zebrafish xenograft model. Our results demonstrate that Hsp90 is a novel target for stromal-based therapy to modulate proinvasive molecular crosstalk within the tumor microenvironment. Furthermore, S06 represents a new class of Hsp90 inhibitor and is an attractive candidate for anticancer drug development.

INTRODUCTION

Forward chemical genetics uses chemical libraries to identify phenotypic changes and target specific proteins (Schreiber, 1998). Small molecules replace the mutation-inducing agents (e.g., DNA adducts and X-ray irradiation) used in classical genetics. Nonetheless, the promise of chemical genetics is restricted by experimental difficulties associated with target identification, such as conjugating the active lead compound to an affinity matrix without reducing biological activity. To overcome this problem, chemically tagged small-molecule libraries have been developed that possess a built-in linker (Kim and Chang, 2007). The presence of a linker in the chemical library prior to biological screening reduces the need for laborious structure-activity relationship studies.

Forward chemical genetics has been used in cancer research to discover new drugs and novel drug targets (Nakai et al., 2006; Williams et al., 2008). In the past decade, cancer research has increasingly focused on the tumor microenvironment as a key regulator of carcinoma progression (Bissell and Hines, 2011; Kolata, 2009; Langley and Fidler, 2011). The tumor microenvironment is a complex milieu consisting of various cell types, extracellular matrix macromolecules, and cell signaling molecules. Among them, carcinoma-associated fibroblasts (CAFs) have been recognized as prominent modifiers of tumor initiation and progression (Kalluri and Zeisberg, 2006). CAFs communicate with other types of cells including cancer cells, playing an active role in carcinogenesis by increasing tumor cell growth, angiogenesis, and invasiveness through secretion of chemokines (Jung et al., 2010; Orimo et al., 2005). This molecule-based communication is termed "crosstalk" (Condon, 2005). Therefore, the molecular crosstalk between cancer cells and CAFs has emerged as a potential target for new drug development.

Recently, we have shown that the chemokine (C-C motif) ligand 7 (CCL7) is a key modulator of the proinvasive crosstalk between CAFs and oral squamous cell carcinoma (OSCC) (Jung et al., 2010). As a next approach, the current study attempted to discover novel inhibitors of CAF crosstalk with carcinoma cells by a forward chemical approach. We chose to study OSCC in our model, because it comprises over 90% of human head and neck cancers (Vokes et al., 1993) and because it is relatively easy to obtain sufficient numbers of biopsy specimens for primary cell culture. A collagen-insert-based transwell culture system was used to screen a tagged triazine library of small molecules for modulators of the cytokine-based crosstalk between CAFs and carcinoma. Using this approach, we identified a novel triazine compound, S06, as an inhibitor of carcinoma-CAF crosstalk, targeting the molecular chaperone heat-shock protein 90 (Hsp90).

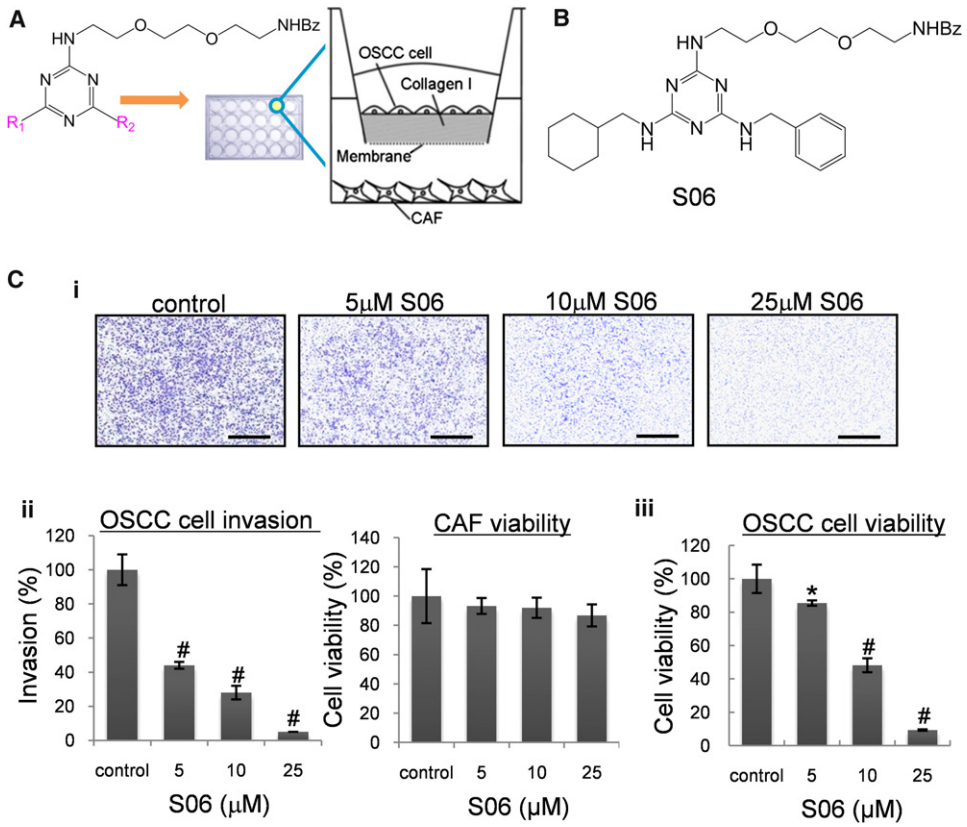

Figure 1. Novel Triazine S06 Inhibits OSCC Cell Invasion Induced by CAF

(A) Screening system used to identify novel regulators of cancer cell invasion. A tagged chemical library of 1040 benzoyl-capped triazines was used for screening. Five μM of each triazine compound was added to the lower chamber of a transwell-based cell-culture system containing YD10B OSCC cells and CAFs separated by an 8-μm porous collagen-coated insert. After 48 hr incubation, the inserts were removed and stained with crystal violet to quantify YD10B invasion.

(B) Chemical structure of S06.

(Ci) Crystal violet staining of YD10B cells invaded onto the transwell inserts. Treatment with increasing concentrations of S06 for 48 hr reduced YD10B invasion in a dose-dependent manner. Scale bar = 200 μM.

(Cii) Quantification of the inhibitory effect of S06 on YD10B invasion. $^{\#}p < 0.01$ compared to control. Cell viability of CAFs cocultured in the system was measured using MTT assay after the S06 treatment.

(Ciii) S06 treatment reduced YD10B cell viability in a dose-dependent manner in the coculture system. CAFs and YD10B cells were cultured in the upper and lower chambers, respectively, of 24-transwell plates containing collagen-coated 1-μm-pore transmembrane filters. S06 (5, 10, and 25 μM) was added to the coculture and cell viability was assessed by MTT assay after 48 hr incubation. $^{*}p < 0.05$ compared to control; $^{\#}p < 0.01$ compared to control.

Data in Figures Ci–Ciii are representative of three independent experiments (mean ± SD of triplicate assays). DMSO served as a control. See also Figure S1.

RESULTS

Identification of a Triazine Compound, S06, as a Novel Inhibitor of OSCC Invasion Induced by CAFs

In our previous study (Jung et al., 2010), we found that CAFs greatly increase OSCC cell invasion in a transwell-based coculture system by secreting proinvasive and promigratory signals in response to the cancer cells. To discover novel inhibitors that inhibit the proinvasive crosstalk between cancer cells and CAFs, we employed a screening assay based on the 24-transwell coculture system. CAFs were added to the bottom chamber 16 hr prior to seeding YD10B OSCC cells. Triazine library compounds were then added to the transwell at 5 μM (final concentration) for 48 hr. To rule out the compounds that exhibit nonspecific toxicity against CAFs, we carried out the MTT assay using the cocultured CAFs after 48-hr drug treatment.

The chemical structure of the triazine-based small-molecule library is shown in Figure 1A. Also shown is a diagram of the screening system used to identify novel modulators of YD10B OSCC invasion. Screening of this small-molecule library led to the identification of S06 as a novel inhibitor of YD10B cell invasion induced by CAFs (Figure 1B).

S06 inhibited YD10B invasion in a dose-dependent manner without affecting CAF viability (Figures 1Ci and 1Cii). S06 also reduced YD10B cell viability in the co-culture system (Figure 1Ciii). However, S06 had a proportionally greater effect on YD10B invasion compared to viability. For example, S06 reduced YD10B cell invasion by 44 ± 2% at the 5 μM concentration at which YD10B cell viability (85 ± 2%) showed only a slight reduction (shown in Figures 1Cii and 1Ciii), indicating that the anti-invasive effect of S06 was resulted from modulating proinvasive signals from CAFs rather than inhibiting cancer cell

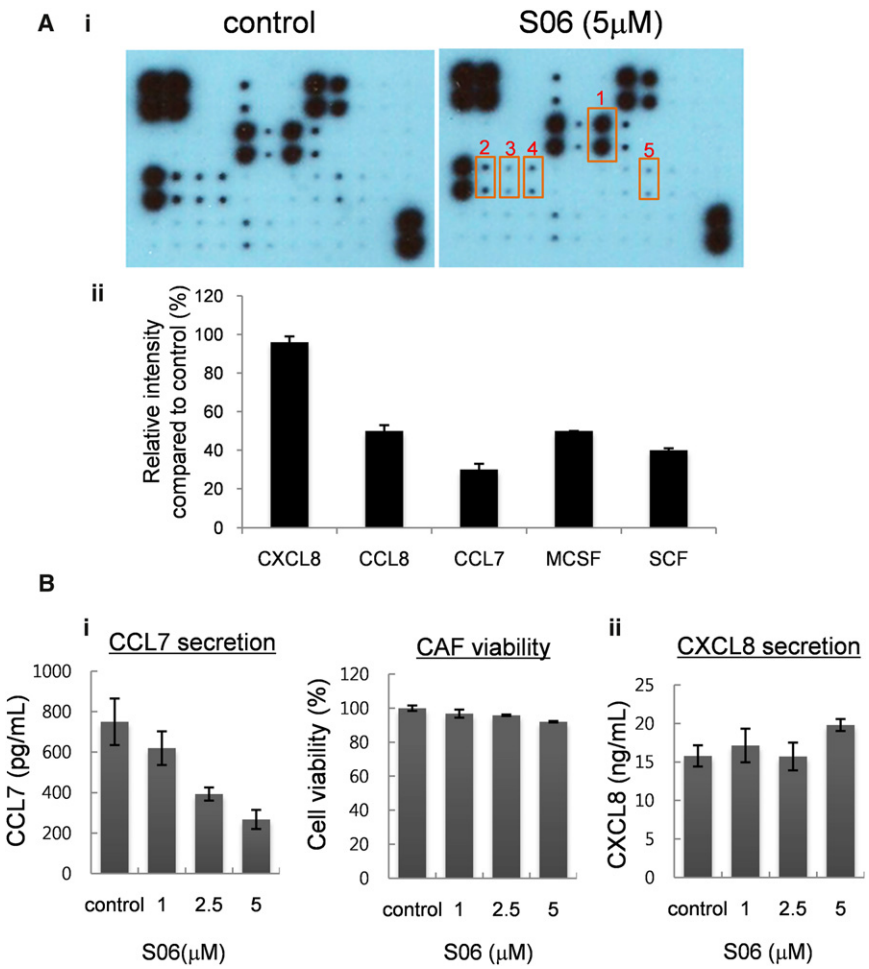

Figure 2. S06 Decreases the Secretion of Proinvasive Chemokines by CAF

(Ai and Aii) Cytokine array analysis showed that 5 μM S06 treatment of CAFs for 24 hr reduced the expression of proinvasive cytokines MCP-2/CCL8 (box 2), MCP-3/CCL7 (box 3), MCSF (box 4), and SCF (box 5). However, expression of the proinvasive cytokine IL-8/CXCL8 (indicated by box 1) remained unchanged. Data shown are representative of two independent experiments. See also Figure S2.

(Bi and Bii) CAFs (2×10^4 cells/well) were cultured with YD10B (2×10^4 cells/well) in the presence and absence of S06 (1, 2.5, and 5 μM) for 24 hr in 24-transwell plates. DMSO served as a control. Data are representative of three independent experiments (mean ± SD of triplicate assays). (Bi) ELISA confirmed that treatment with S06 for 24 hr reduced the secretion of CCL7 by CAFs. Treatment with S06 had no significant effect on CAF viability. (Bii) ELISA confirmed that treatment with S06 for 24 hr had no significant effect on CXCL8 secretion by CAFs, which is in accordance with the cytokine antibody array data shown in Figure 2A.

viability. Therefore, we concluded that S06 inhibits OSCC cell invasion by perturbing proinvasive properties of CAFs, in addition to inhibiting cancer cell proliferation. Furthermore, S06 exhibited anti-invasive effects on other OSCC cell lines (HSC-2 and Ca9.22) in a dose-dependent manner (Figure S1 available online).

S06 Reduced the Secretion of Proinvasive Chemokines by CAFs

To determine the effect of S06 on cytokine secretion by CAF, cytokine antibody array analysis was performed using CAF-conditioned media, treated with or without 5 μM S06. We found that S06 inhibited the secretion of proinvasive and pro-migratory chemokines, such as chemokine (C-C motif) ligand 7 (CCL7/MCP-3) and chemokine (C-C motif) ligand 8 (CCL8/MCP-2) (Figures 2Ai, 2Aii, and S2). In addition, macrophage colony stimulating factor (MCSF), and stem cell factor (SCF), known as cancer-promoting cytokines (Filderman et al., 1992; Huang et al., 2008) also showed decreased secretion in response to treatment with S06. Recently, CCL7 has been shown to be a key mediator of OSCC invasion (Jung et al., 2010). Enzyme-linked immunosorbent assay (ELISA) confirmed that S06 also inhibited the secretion of CCL7 by CAFs stimulated with YD10B culture, without affecting CAF cell viability (Figure 2Bi). In addition, ELISA confirmed that S06 had no effect on the secretion of CXCL8 by CAFs stimulated with YD10B culture (Figure 2Bii), which is also in accordance with the result obtained from the cytokine antibody array.

S06 Targets Hsp90 in Both OSCC Cells and CAFs

Affinity chromatography using an S06-conjugated matrix showed that Hsp90α and tubulin were the specific targets in YD10B OSCC cells (Figure 3Ai). However, S06 did not affect tubulin polymerization (Figure S3A), indicating that tubulin is not an active target. The Hsp90α peptide fragments identified by mass spectrometry are shown in Figure 3Aii. Competition binding studies using free S06-A (without the linker portion, structure and activity shown in Figure S3B) confirmed that S06 binds to Hsp90α and TNF receptor-associated protein 1 (TRAP-1, a 75-kD paralog of Hsp90α containing a conserved N-terminus) in YD10B cells (Figure 3B). An identical result was found in CAF (Figure 3C). In support of this result, an S06-conjugated matrix could also bind to recombinant Hsp90α (Figures 3Di and 3Dii). It was found that S06 binds to the N-terminus of Hsp90α in a dose-dependent manner (Figures 3Ei and S3D). Binding of the S06-conjugated matrix to the Hsp90α N-terminus was confirmed by competition binding analysis using free S06-A and S06 (Figures 3Eii and S3E).

Inhibition of Hsp90 in CAF Decreased CCL7 Secretion and Reduced Cancer Cell Invasion

To validate Hsp90 as a cellular target of S06 in CAFs, we carried out knockdown of Hsp90 expression in CAFs using siRNA. Western blotting was used to confirm Hsp90 knockdown by siRNA (64% expression compared to control; Figure 4Ai).

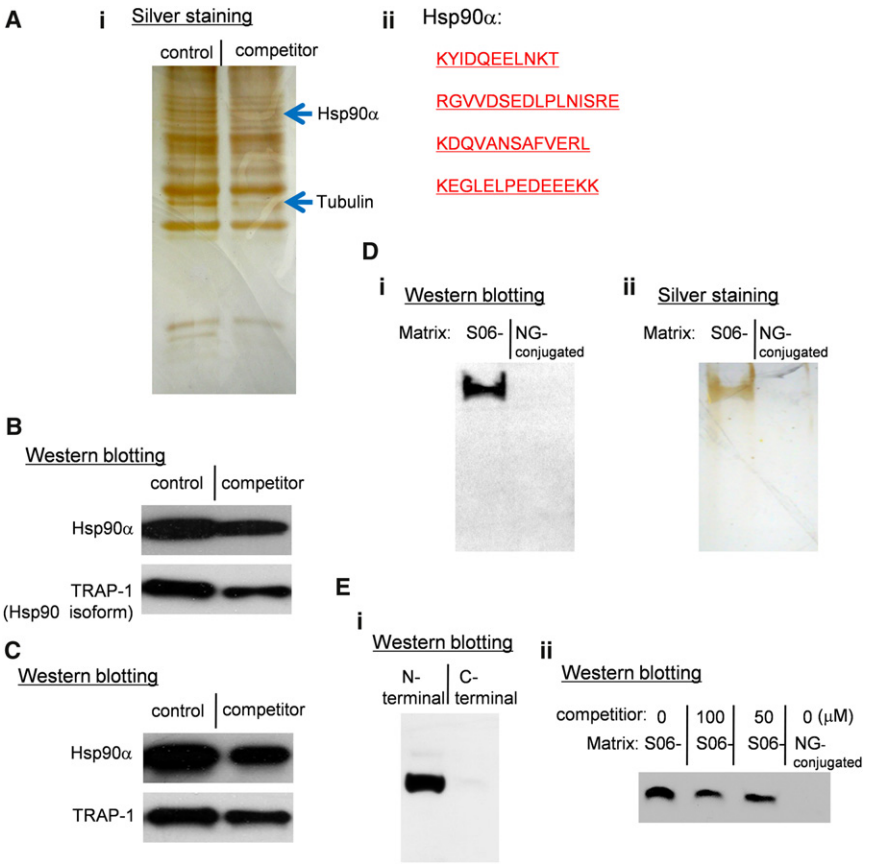

Figure 3. Affinity Pull Down Assays Identified Hsp90 as a Target of S06

(Ai) Drug target study for the S06 in YD10B cell lysate. Eluted proteins were separated by 10% SDS-PAGE. Lanes: competitor, conjugated affinity matrix in the presence of 100 μM S06-A; control, conjugated affinity matrix in the absence of S06-A. S06-A is a derivative of S06 with the linker moiety removed.

(Aii) Hsp90α proteins identified by MALDI TOF MS/MS analysis.

(B) Competition studies for the S06 in YD10B cell lysate. Eluted proteins were blotted and probed with antibodies against Hsp90α and TNF receptor-associated protein 1 (TRAP-1, a 75 kD paralog of Hsp90α containing a conserved N-terminus). Lanes: competitor, conjugated affinity matrix in the presence of 100 μM S06-A; control, conjugated affinity matrix in the absence of S06-A.

(C) Competition binding studies for the S06 in CAF cell lysate. Eluted proteins were blotted and probed with antibodies against Hsp90α and TRAP-1. Lanes, Competitor, conjugated affinity matrix in the presence of 100 μM S06-A; control, conjugated affinity matrix in the absence of S06-A.

(D) S06 affinity matrix binds to full-length human recombinant Hsp90α tagged with histidine.

(Di) Eluted proteins were separated on a 10% SDS-PAGE gel, blotted, and probed with an antihistidine antibody. Lanes: NG−, inactive compound N10-conjugated affinity matrix (chemical structure of N10 is shown in Figure S3F). S06−, S06-conjugated affinity matrix.

(Dii) Silver staining. Eluted proteins were separated on a 10% SDS-PAGE gel.

(Ei) S06-conjugated affinity matrix was incubated with histidine-tagged N-terminal (amino acids 12–230) or C-terminal (amino acids 539–732) fragments of human Hsp90α. After washing, the eluate was blotted and probed with the histidine-specific monoclonal antibody.

(Eii) Competitive binding of S06 to the N-terminal fragment. S06-conjugated affinity matrix was incubated with histidine-tagged N-terminal fragment with or without S06-A (50 and 100 μM). The eluate was blotted and probed with the antihistidine antibody. NG-conjugated, inactive compound N10-conjugated affinity matrix. See also Figure S3.

Hsp90 knockdown in CAFs reduced invasion of cocultured OSCC cells (56 ± 9% of control cell invasion) and secretion of the key proinvasive chemokine CCL7 (67 ± 2.4% compared to control; shown in Figures 4Aii and 4Aiii).

In addition, 17-AAG, a widely-characterized Hsp90 inhibitor, was shown to decrease CCL7 secretion in either CAF monoculture or co-cultured CAF with OSCC cells, inhibiting the cancer cell invasion (Figures 4B and 4C).

Furthermore, Hsp90 inhibition by S06 or 17-AAG treatment was found to inhibit nuclear-factor kappa-light-chain-enhancer of activated B cell (NFκB) activation in CAFs (Figure S4), providing an explanation for the relationship between Hsp90 inhibition and the CCL7 decrease, which are known to be inducible through the NFκB pathway (Thompson and Van Eldik, 2009).

S06 Exhibited Less Toxicity against Hepatocytes Compared to 17-AAG

Antibiotic derivative 17-AAG is a widely characterized Hsp90 inhibitor that is in clinical trials for young patients with certain types of leukemia or solid tumors (Schulte and Neckers, 1998; Solit et al., 2007). 17-AAG treatment induced cytotoxicity in YD10B OSCC cells (Figure S5B). However, 17-AAG is also known to cause hepatotoxicity (Guo et al., 2008), and treatment of primary C57BL/6 hepatocytes with 5 μM 17-AAG for 48 hr induced cytoplasm retraction. In contrast, the primary hepatocytes treated with the same concentration of S06 appeared normal (Figure S5A). MTT assay confirmed that S06 treatment up to 20 μM concentration does not induce hepatotoxicity, in contrast to 17-AAG, as shown in Figure 5A. IC_{50} of 17-AAG was 0.389 μM for 48-hr treatment: only slightly higher (2.6-fold) than the EC_{50} for YD10B OSCC cells under the same treatment (0.148 μM, Figure S5B); however, IC_{50} of S06 was 65.4 μM: 13.3-fold higher than the EC_{50} for YD10B OSCC cells (4.9 μM, Figure S5C).

S06 Inhibits OSCC Cell Migration and Metastasis In Vivo

Zebrafish (*Danio rerio*) is gaining increasing research prominence as a model for measuring cancer cell progression (Liu and Leach, 2011; Rouhi et al., 2010). DiI-labeled OSCC cells were injected into the zebrafish yolk sac at 48 hpf (Figure S5D) and treated with 5 μM S06, 150 nM 17-AAG, or 50 nM paclitaxel in 96-well plates. The concentrations 5 μM S06 and 150 nM 17-AAG were chosen for this study because they showed no toxicity in the hepatocyte culture, as shown in Figure 5A. Paclitaxel served as a positive control. Four days later, embryos treated with 5 μM S06 showed reduced OSCC cell migration

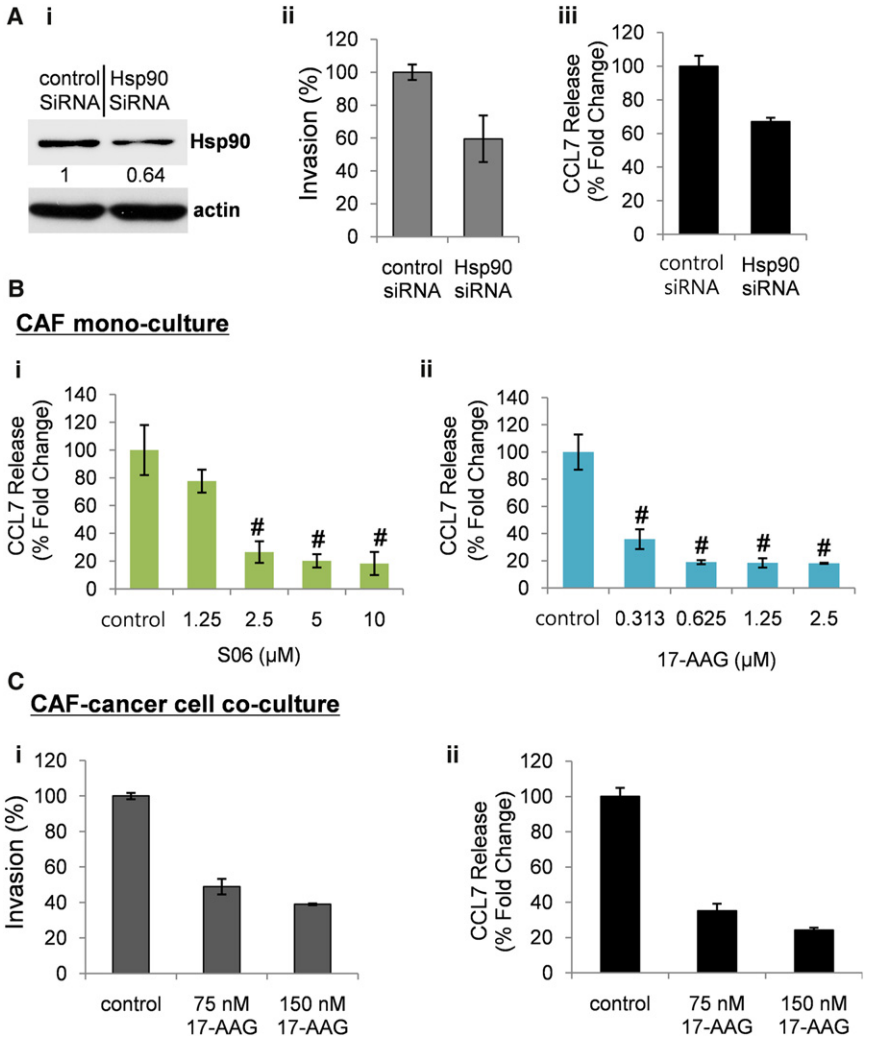

Figure 4. Inhibition of Hsp90 Decreased CCL7 Secretion and Reduced Cancer Cell Invasion in Co-Culture System

(A) Effect of Hsp90 gene knockdown in CAFs on CCL7 secretion and induction of cancer cell invasion. CAFs were treated with Hsp90 siRNA for 48 hr and then cocultured with YD10B cancer cells in the transwell system for 24 hr. Data are representative of three independent experiments (mean ± SD of triplicate assays).

(Ai) Immunoblotting to confirm that treatment of CAFs with Hsp90 siRNA for 48 hr reduced the expression of Hsp90. Numbers beneath each blot show the fold change in band intensity; actin was used as a loading control for normalization.

(Aii) Gene knockdown of Hsp90 in CAFs reduced the invasion of cocultured YD10B cells. (Aiii) Gene knockdown of Hsp90 in CAFs reduced the secretion of CCL7 by CAFs.

(Bi and Bii) Comparison of CCL7 secretion by CAFs after treatment with S06 (i) or the widely studied anticancer drug 17-AAG (ii), which also targets Hsp90. CAFs were treated with drug for 48 hr. $^{\#}p < 0.01$ compared to untreated cells. Data are representative of three independent experiments (mean ± SD of triplicate assays). DMSO served as a control.

(C) 17-AAG treatment reduced CCL7 release from CAFs increased by cocultured OSCC cells and decreased OSCC cell invasion toward cocultured CAFs. 17-AAG at two concentrations, 75 nM and 150 nM, was treated in the transwell-based CAF-YD10B coculture. Data are representative of three independent experiments (mean ± SD of triplicate assays). DMSO served as a control. See also Figure S4.

(Ci) At 24 hr after treatment, YD10B cell invasion was measured by counting transmigrated cells through transwell filters.

(Cii) The culture media were collected for CCL7-specific ELISAs.

and metastasis from the injection site (Figure 5B). Of the xenoplanted fish, 48 ± 6% showed cell migration and metastasis after S06 treatment, whereas 63 ± 3% showed cell migration and metastasis in the untreated control group. A similar reduction in numbers of xenoplanted fish (38 ± 8%) showed cell migration and metastasis in zebrafish treated with 50 nM paclitaxel (a tubulin stabilizing drug used in cancer chemotherapy [Wani et al., 1971]). However, 17-AAG was found to be less effective than S06 (54 ± 4%). Representative OSCC-cell xenoplanted fish and S06-treated xenoplanted fish are shown in Figure 5Bii.

DISCUSSION

The tumor microenvironment is a major focus for understanding cancer progression (Guise, 2010; Witz, 2008). However, there is no previous published report exploiting new drugs targeting the molecular crosstalk in this microenvironment. To our knowledge, in the present study, we discovered, for the first time, a key regulator of tumor-fibroblast crosstalk in the microenvironment via a forward chemical genetic approach. Moreover, we also present S06 as a novel class of Hsp90 inhibitor that possesses therapeutic potential for drug development, based on low hepatotoxicity and promising animal model data.

The transwell cell culture system used in our study is well suited for identifying new modulators of the tumor microenvironment. CAFs, recognized as a main cell type of the tumor stroma, were cocultured with cancer cells to induce cancer cell invasion. Collagen-type-I-coated porous membrane separated the two types of cells, allowing proinvasive crosstalk mediated by soluble factors, rather than direct cell-cell contact. The compound of interest can be added to the culture media while the cell populations remain physically separated by the collagen matrix and porous membrane insert. Cancer cell invasion can be simply measured by staining cells that are retained by the membrane. To rule out compounds that exhibit nonspecific cytotoxicity, CAFs can be tested for viability after drug treatment. For screening, the linker-tagged benzoyl-capped small-molecule library of triazines was chosen because of previous successes using this library, such as the dissection of cellular pathways relating to pigmentation and insulin signaling (Min et al., 2007; Williams et al., 2004). Our screening system is also suitable for

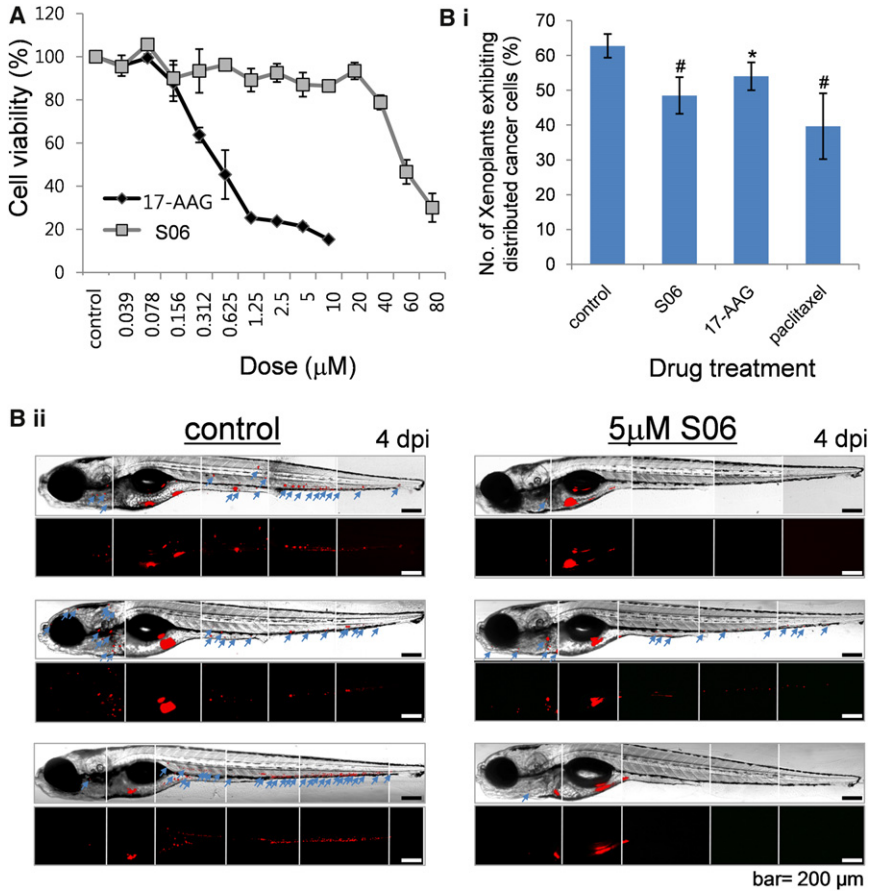

Figure 5. S06 Inhibits OSCC Cell Metastasis In Vivo

(A) MTT assay analysis showed that treatment with novel Hsp90 inhibitor S06 did not adversely affect hepatocyte viability. In contrast, hepatocytes treated with the known Hsp90 inhibitor 17-AAG showed a significant reduction in viability 48 hr after AAG treatment. Data shown are representative of three independent experiments (mean ± SD of triplicate assays). DMSO served as a control.

(Bi) Treatment of YD10B-xenotransplanted zebrafish with S06, 17-AAG, or paclitaxel for 96 hr reduced the number of embryos showing migration and metastasis (distributed cancer cells). Error bars indicate the mean ± SD; *$p < 0.05$ compared to control; #$p < 0.01$ compared to control fish; data are the mean of three independent experiments. DMSO served as a control.

(Bii) Three representative embryos are shown for each treatment group. Microtumor foci are designated by arrows. See also Figure S5.

further optimization, such as colorimetric assessment of tumor cell invasion (Saito et al., 1997).

The tumor microenvironment exerts its influence on cancer progression through an extremely complex network of cytokines, chemokines, and extracellular matrix components (Kalluri and Zeisberg, 2006). Thus, it is especially important to identify key regulators within this environment. An earlier report from our group described the chemokine CCL7 as a pivotal component of the carcinoma microenvironment (Jung et al., 2010). Cytokine antibody array analysis showed that S06 produced a fairly specific effect on the stromal fibroblast-carcinoma cell microenvironment, with just 4 of 44 cytokines tested being influenced by S06 treatment, one of which was CCL7 (Figure 2). The other three downregulated cytokines (CCL8, MCSF, and SCF) have also been shown to be upregulated in the tumor microenvironment and contribute to tumor invasion (Filderman et al., 1992; Huang et al., 2008; Proost et al., 1998).

To determine whether S06 inhibits cancer cell proliferation, we treated S06 to carcinoma cell mono-cultures and carried out cell viability tests. Induction of cytotoxicity by S06 was studied in OSCC cell mono-culture, because CAFs have been shown to enhance cancer cell survival and proliferation (Orimo et al., 2005). S06 inhibited proliferation in a range of carcinoma cell lines from different tissues, as well as three different OSCC cell lines (Figure S6A). In contrast, S06 did not induce cytotoxicity in primary cultures of human normal epithelial cells (Figure S6A). Annexin V/carboxyfluorescein diacetate staining and annexin V/propidium iodide flow cytometric analysis confirmed that S06 induces apoptosis in carcinoma cells (Figures S6B and S6C).

Furthermore, we have shown that the active cellular target of S06 in both cancer cell and CAFs is the N-terminus, ATPase-binding region of Hsp90 (Figure 3; Figure S3). Hsp90 is a member of a class of proteins referred to as molecular chaperones with key roles in the folding, activation, and assembly of a range of client proteins. Recently, Hsp90 has received great attention as an attractive target in cancer therapy due to its critical role in mediating the maturation and stability of a variety of cancer-associated proteins (Li et al., 2009; Pearl and Prodromou, 2000; Sharp et al., 2007). However, its role in tumor-associated stromal cells, implicating a new paradigm for cancer therapy through stromal cell inhibition, has not been reported. In the present study, S06 inhibits tumor invasion by disrupting the chaperone function of Hsp90 expressed in CAFs, causing incorrect trafficking of signaling pathway proteins, such as NFκB, that regulate expression of proinvasive chemokines, including CCL7 (Qing et al., 2007; Thompson and Van Eldik, 2009). In addition, continuous perturbation of Hsp90 function in cancer cells eventually produces apoptosis via disruption of the molecular mechanisms required for their survival. S06 and 17-AAG treatments of OSCC cells reduced the expression of Hsp90 client proteins that are protective against apoptosis; Bcl-xL, survivin, and Akt (Figure S6D). It should be noted that previous studies showed Hsp90 inhibitors can selectively kill cancer cells compared to normal cells (Kamal et al., 2003). In addition, a large number of proteins in tumor cells are dependent upon Hsp90 protein folding machinery for their maturation (Donnelly and Blagg, 2008). A schematic of the S06 mode of action is illustrated in Figure 6.

To our knowledge, our study presented herein is the first use of forward chemical genetics to discover an Hsp90 inhibitor

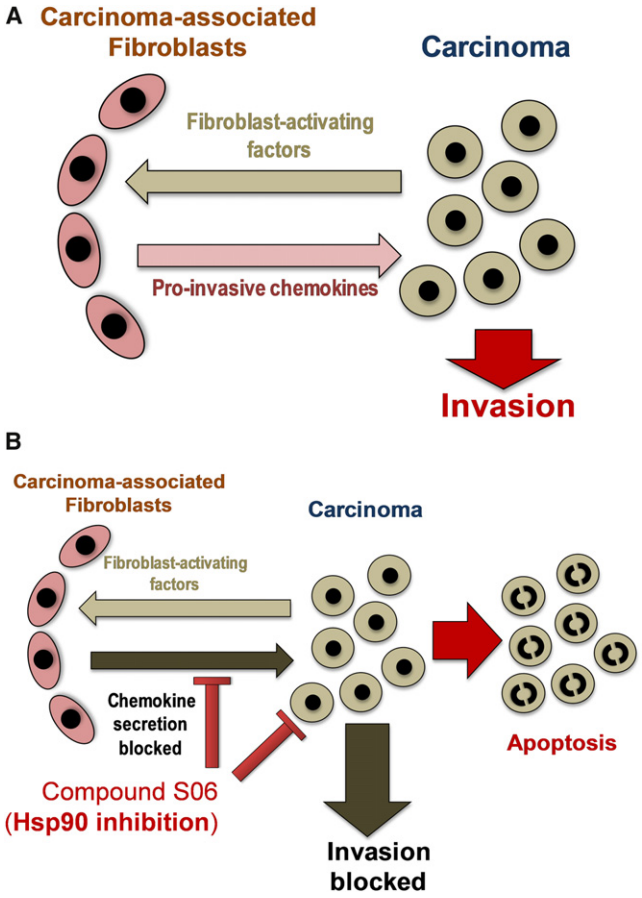

Figure 6. Schematic Diagram of Tumor Microenvironment Modulation by S06

(A) Oral carcinoma cells activate carcinoma-associated fibroblasts by secreting cytokines, such as interleukin-1α (Jung et al., 2010). Activated fibroblasts secrete chemokines, such as CCL7, that promote carcinoma invasion.

(B) S06 targets the molecular chaperone Hsp90 to block carcinoma progression. Secretion of proinvasive chemokines from activated fibroblasts is inhibited by S06 treatment through Hsp90 inhibition. S06 destabilizes anti-apoptotic Hsp90 client proteins expressed in carcinoma cells, resulting in programmed cell death of the carcinoma cells. See also Figure S6.

(S06) via screening for modulators of cancer-cell crosstalk within the tumor microenvironment. Using this approach, we have been able to show that S06 perturbs key chemokine signaling between carcinoma cells and stromal fibroblasts to reduce carcinoma invasion by inhibiting Hsp90 expressed in the fibroblasts. We believe our methodology is very useful for discovering novel anticancer agents, because S06 perturbs molecular crosstalk within the tumor microenvironment without inducing significant toxicity in normal cells (Figure S6A). Furthermore, our study showed that S06 does not induce hepatotoxicity at a concentration of 20 μM, while OSCC cell viability was decreased to almost 0%. In contrast, 17-AAG does not induce hepatotoxicity at 156 nM concentration, but OSCC cell viability is decreased to only 54% under the same conditions (Figures 5A and S5B). Further comparative studies of S06 and 17-AAG could include assessment of chaperone function; because a number of proteins upregulated in tumor cells, such as Met, Akt, and STAT3, are Hsp90 client proteins (McCleese et al., 2009; Walter and Buchner, 2002). 17-AAG efficacy has been linked to P-glycoprotein expression and metabolism by NAD(P)H dehydrogenase (quinone) (Sharp et al., 2007), and it would be interesting to test whether the function of S06 is also susceptible to these factors.

We have validated the therapeutic potential of S06 in the zebrafish animal model. Over the past decade, zebrafish have gained increasing popularity in cancer research (Stern and Zon, 2003; Taylor and Zon, 2009). This is not only due to economic and practical considerations; zebrafish also allow in vivo visualization of cell migration, high-resolution imaging of transplanted tumor cells, and analysis of interactions between cancer and host cells. These features are not available in mammalian models. Incubation of recipient animals with 5 μM S06 was sufficient to inhibit OSCC cell migration and metastasis without producing toxic effects in the host. It has been shown that human tumor cell characteristics, such as relative migration capabilities, can be replicated in the zebrafish transplantation model (Haldi et al., 2006; Marques et al., 2009). Thus, based on the inhibition of migration and metastasis in this animal model (Figure 5B), S06 is a good candidate for further development as an anticancer therapeutic.

Considering the current, intense research effort focused on dissecting the main regulators of molecular crosstalk, we believe that our approach provides an excellent methodology for dissecting this crosstalk and providing promising therapeutic agents. Our protocol could be expanded to include other types of tumor-associated cells, such as tumor-associated macrophages and pericytes, or multiple cell populations. Thus, our approach provides a convenient system for comprehensive analysis of the tumor microenvironment and identifying novel drug targets.

SIGNIFICANCE

The tumor microenvironment is now acknowledged as a key regulator of cancer progression. However, we have not fully characterized the important signaling pathways that control tumor cell responses within the microenvironment. This hampers drug development for blocking cancer metastasis. To our knowledge, our study presents a new approach to forward chemical genetics: using screening to discover new molecular targets that control cellular crosstalk in the tumor microenvironment. To our knowledge, we have shown for the first time that Hsp90 is an important drug target for blocking the cellular crosstalk that promotes tumor invasion. Furthermore, we have shown that our small molecule inhibitor of Hsp90, termed compound S06, is a promising new drug candidate for blocking cancer invasion. Compound S06 shows reduced hepatoxicity compared to a known Hsp90 inhibitor, 17-AAG, which is currently undergoing clinical evaluation in cancer and leukemia patients. Moreover, we show that compound S06 is effective at blocking tumor cell metastasis in an animal model. Our work is significant for chemical biology, because we have used chemical tools to dissect a key regulatory pathway in the tumor microenvironment. This microenvironment is a milieu

of multiple cell types (including endothelial cells, stromal fibroblasts, macrophages, and pericytes, in addition to cancer cells) secreting multiple signaling molecules. Our approach is important, because we have developed a chemical screen that models a key interaction within this milieu: tumor cell crosstalk with stromal fibroblasts. Our animal model data validate our screening system and the discovery of Hsp90 as a regulator of tumor cell invasion. Thus, we have shown that forward chemical genetics can be used to unravel the complex signaling network in the tumor microenvironment; providing new drug targets and chemical probes to further our understanding of cancer initiation and progression.

EXPERIMENTAL PROCEDURES

Antibodies

The following antibodies were purchased from Cell Signaling (Beverly, MA, USA): cleaved Poly (ADP-ribose) polymerase (PARP), B cell lymphoma-extra large (Bcl-xL), survivin, and protein kinase B (Akt). Antibodies against caspase-3 were purchased from R&D systems (Minneapolis, MN, USA) and Cell Signaling. An antibody against Hsp90α was purchased from Abcam (Cambridge, MA, USA). An antibody against tumor necrosis factor (TNF) receptor-associated protein 1(TRAP-1) was purchased from Santa Cruz Biotechnology (Santa Cruz, CA, USA). Antibodies against actin and histidine were purchased from Sigma-Aldrich (St. Louis, MO, USA).

Cell Culture

CAFs were derived from the surgical specimen of an OSCC patient. Informed consent for this study was given by the patient to Yonsei University College of Dentistry, Seoul, Republic of Korea. CAFs were selected by Versene solutions (0.1 g EDTA and 2 ml glucose in 500 ml PBS) from explanted cancer tissues. The isolated fibroblasts were characterized by immunohistochemical staining with anti-vimentin (1:100 dilution, DAKO, Tokyo, Japan) and anti-α-smooth muscle actin (1:50 dilution, Sigma, St. Louis, MO), along with comparison to normal fibroblasts, as previously described (Jung et al., 2010). CAFs were cultured in a 3:1 ratio of Dulbecco's modified Eagle's medium (DMEM; GIBCO BRL, Baltimore, MD, USA) and nutrient mixture F-12 Ham (HAM's-F12; GIBCO BRL), supplemented with 10% FBS and 1% penicillin/streptomycin. The established OSCC cell line YD10B was obtained from the Korean Cell line Bank (Seoul, Republic of Korea) and cultured as described (Che et al., 2006). The OSCC cell lines HSC-2 and Ca9.22 were gifts from Professor T. Muramatsu, Toyko Dental College, Japan, and maintained in DMEM: Ham's-F12 (3:1) culture media, supplemented with 10% FBS and 1% penicillin/streptomycin. The breast cancer cell lines MDA-MB-231, MDA-MB-435, and MCF-7 were obtained from the American Type Culture Collection (ATCC) and cultured in DMEM supplemented with 10% FBS and 1% penicillin/streptomycin. The PC-3 prostate cancer cell line was maintained in Ham's-F12 supplemented with 10% FBS and 1% penicillin/streptomycin. The A549 lung cancer cell line was maintained in MEM supplemented with 10% FBS and 1% penicillin/streptomycin. The colon cancer cell lines HT29 and DLD1, and NCI-H460 lung cancer cell lines were maintained in RPMI1640 supplemented with 10% FBS and 1% penicillin/streptomycin. PC-3, A549, NCI-H460, HT29, and DLD1 were gifts from Professor Sun-Young Ra, Yonsei University College of Medicine, Republic of Korea.

Hepatocytes were harvested from 6- to 8-week-old male C57BL/6 mice using in situ collagenase perfusion, as described (West et al., 1989). All cells were cultured at 37°C in an atmosphere containing 5% CO_2.

Cancer Cell Invasion Assay

To evaluate invasive activity, we used a modified transwell invasion assay (Youngs et al., 1997). Using 24-transwell plates (Corning, Corning, NY, USA), the inserts containing filters with pore size 8 μm were coated with collagen type I (45 μg/30 μl/well) for invasion assay. Briefly, 2 × 10^4/well CAFs were seeded in the lower well chambers for inducing cancer cell invasion. After 24 hr, 2 × 10^4/well OSCC cells were placed in the upper transwell chambers with porous filters. The cancer cells that penetrated the filter were fixed and stained with 0.25% crystal violet. Cell invasion was quantified by counting the invaded cells, which were counted in five separate microscopic fields (100×) per filter, and the mean values per filter (±SD) were calculated from three replicate filters.

Measurement of Cell Proliferation

Cell proliferation was measured using the MTT assay, as previously described (Mosmann, 1983). Briefly, cells were seeded in a 96-well culture plate, 16 hr before addition of the drug. MTT absorbance was read at 540 nm using a microplate reader (VersaMax, BioRad, Hercules, CA, USA).

Chemical Library Screening

A tagged chemical library of 1040 benzoyl-capped triazines (Kim and Chang, 2007) was used for screening. CAFs were seeded in the lower chamber of a transwell at a density of 2 × 10^4 cells/well. After overnight incubation, the cell culture medium was changed to a serum-free medium and 5 μM of each compound was added to the lower chamber. YD10B OSCC cells (2 × 10^4) were then added to the upper, collagen-coated chamber (Figure 1A). After 48 hr incubation, OSCC invasion was measured by staining with 0.25% crystal violet and cell counting. Cytotoxicity of S06 against YD10B cells or CAFs in the coculture system was assessed by MTT assay, employing transwells equipped with a filter of pore size 0.4 μm, which blocked cell penetration through the filter, although co-cultured cells could still influence each other.

Cytokine Antibody Array Analysis

The sandwich ELISA human cytokine antibody array was purchased from RayBiotech (Norcross, GA, USA). CAF cells (2 × 10^5) were cultured in T25 cm^2 tissue culture flasks overnight and the medium was changed to serum-free DMEM/F12 (3:1) medium with DMSO (vehicle) or 5 μM S06 after three washes with PBS. After 24 hr incubation, the supernatants were collected and examined according to the manufacturer's instructions.

Enzyme-Linked Immunosorbent Assay

CCL7/MCP-3 and IL-8/CXCL8 in cell culture supernatants were quantified by sandwich ELISA, using kits purchased from R&D Systems (Minneapolis, MN, USA).

Isolation and Identification of Cellular Targets

Proteins were extracted from YD10B OSCC cells or CAFs by incubation with extraction buffer (1 mM $CaCl_2$, 150 mM NaCl, 10 mM Tris, pH 7.4, 1% Triton X-100, and 1 mM PMSF plus one tablet of protease inhibitor cocktail (Roche, Basel, Switzerland) per 10 ml buffer) for 5 min on ice. Crude lysate was centrifuged at 10,000 rpm for 10 min. The protein concentration of the supernatant was measured by Bradford assay (Bio-Rad, Hercules, CA, USA) and adjusted to a final concentration of 1 μg/μl prior to affinity chromatography. Twenty-five μl of agarose affinity matrix conjugated compound was washed with 1 ml bead buffer (10 mM Tris, pH 7.4, 5 mM NaF, 250 mM NaCl, 5 mM EDTA, 5 mM EGTA, and 0.1% Triton X-100 plus one tablet of protease inhibitor cocktail per 10 ml buffer). Matrices were incubated with 100 μl of 200 μg protein extract plus an identical volume of bead buffer at room temperature. For studies of competition drug binding to a cellular target, the competitor was added to the mixture of protein extract/bead buffer and incubated at room temperature for 30∼60 min prior to incubation with the matrix. The supernatant containing unbound proteins was removed by centrifugation and the matrices were washed seven times with 1 ml bead buffer. Proteins bound to the matrices were eluted by incubation with 80 μl 2× Laemmli buffer (Bio-Rad) at 95°C for 3 min. Eluted proteins were separated by 10% SDS-PAGE and visualized by silver staining kit (GE Healthcare, St. Giles, UK). Prominent protein bands specific to active matrices were excised from each gel and identified by MALDI-TOF mass spectrometry (Korea Research Institute of Standards and Science, Daejeon, Republic of Korea).

Western Blot Analysis

Proteins were harvested and separated by 8%–12.5% SDS-PAGE and transferred onto 0.45 μm polyvinylidene fluoride (Pall, Port Washington, NY,

USA). Densitometry was carried out using Multi Gauge V3.0 software (Fujifilm, Tokyo, Japan).

Expression and Purification of Recombinant Proteins

The full length (1–732), N-terminal domain (12–230), or C-terminal domain (539–732) of the human Hsp90α tagged with histidine was expressed in *Escherichia coli* BL21. These proteins were purified using a previously described method (Tropea et al., 2009). Ni-NTA-agarose beads (QIAGEN, Venlo, Netherlands) were used for purification. Eluted protein concentrations were determined using the Bio-Rad protein assay kit.

siRNA-Mediated Gene Silencing

Hsp90 and control siRNAs were purchased from Santa Cruz Biotechnology (Santa Cruz, CA, USA). CAFs were seeded in six-well plates at a cell density of 1×10^5 cells/well. CAFs were transfected with 80 pmol of siRNA 24 hr after seeding, following the manufacturer's protocol. CAFs were used for experiments 48 hr after transfection. Invasion assay and CCL7-ELISA were performed after 24 hr co-culture of the siRNA-treated CAFs (2×10^4 cells/well) and YD-10B (2×10^4 cells/well) in the 24-transwell system.

Zebrafish Study of Tumor Cell Metastasis

Wild-type AB zebrafish embryos were obtained using standard mating conditions and staged for cell transplantation at 48 hpf. Embryos were dechorionized using microforceps, anesthetized with tricaine and positioned on their right side on a wet 1.0% agarose pad. YD10B OSCC cells were detached from culture dishes using 0.05% trypsin-EDTA and washed twice with PBS at room temperature. Cells were stained in 2 μg/ml 1,1′-dioctadecyl-3,3,3′,3′-tetramethyl-indocarbocyanine perchlorate (DiI) (Invitrogen, Carlsbad, CA, USA) diluted in PBS and washed with FBS, followed by two washes with PBS and one wash with 10% FBS diluted in PBS. Cells were kept on ice before injection. Approximately 100 tumor cells suspended in 10% FBS were injected into the center of the yolk sac using an injector (PV820 Pneumatic Picopump, World Precision Instruments, Sarasota, FL, USA) equipped with borosilicate glass capillaries. Injected embryos were transferred to a 96-well plate (1 embryo/well) containing the drug of interest diluted in 200 μl E3 media (without methylene blue) and maintained at 31°C. Fifteen embryos were used for each drug treatment group. Embryos were imaged at 4 days post injection (dpi) using an upright fluorescent microscope (Leica, Wetzlar, Germany). Occurrence of cancer cell migration was classified as 100× microscopic observation of more than five microtumor foci that were distinct from the injection site. Care and treatment of animals were conducted in accordance with guidelines established by the Animal Care and Ethics Committees of the Gwangju Institute of Science and Technology (GIST).

Statistical Analysis

Data were analyzed with the SPSS statistical program (version 17.0). One-way ANOVA was used for comparison between multiple groups. Student's t test was used for comparison between two groups. P values of <0.05 were considered significant. Unless otherwise stated, data presented are representative of three independent experiments.

SUPPLEMENTAL INFORMATION

Supplemental information includes six figures and Supplemental Experimental Procedures and can be found with this article online at doi:10.1016/j.chembiol.2011.10.001.

ACKNOWLEDGMENTS

This research was supported by a grant from the National Research Foundation funded by the Korean government (MEST basic science research program NRF-2009-0067894 to D.-W.J.) and a grant from the Priority Research Centers Program through the National Research Foundation of Korea (NRF) funded by the Ministry of Education, Science and Technology (2010-0029702 to J.K.). We also acknowledge the Bioimaging Research Center, Gwangju Institute of Science and Technology, for provision of microscopy facilities.

Received: June 29, 2011
Revised: September 20, 2011
Accepted: October 5, 2011
Published: December 22, 2011

REFERENCES

Bissell, M.J., and Hines, W.C. (2011). Why don't we get more cancer? A proposed role of the microenvironment in restraining cancer progression. Nat. Med. *17*, 320–329.

Che, Z.M., Jung, T.H., Choi, J.H., Yoon, J., Jeong, H.J., Lee, E.J., and Kim, J. (2006). Collagen-based co-culture for invasive study on cancer cells-fibroblasts interaction. Biochem. Biophys. Res. Commun. *346*, 268–275.

Condon, M.S. (2005). The role of the stromal microenvironment in prostate cancer. Semin. Cancer Biol. *15*, 132–137.

Donnelly, A., and Blagg, B.S. (2008). Novobiocin and additional inhibitors of the Hsp90 C-terminal nucleotide-binding pocket. Curr. Med. Chem. *15*, 2702–2717.

Filderman, A.E., Bruckner, A., Kacinski, B.M., Deng, N., and Remold, H.G. (1992). Macrophage colony-stimulating factor (CSF-1) enhances invasiveness in CSF-1 receptor-positive carcinoma cell lines. Cancer Res. *52*, 3661–3666.

Guise, T. (2010). Examining the metastatic niche: targeting the microenvironment. Semin. Oncol. *37* (*Suppl 2*), S2–S14.

Guo, W., Reigan, P., Siegel, D., and Ross, D. (2008). Enzymatic reduction and glutathione conjugation of benzoquinone ansamycin heat shock protein 90 inhibitors: relevance for toxicity and mechanism of action. Drug Metab. Dispos. *36*, 2050–2057.

Haldi, M., Ton, C., Seng, W.L., and McGrath, P. (2006). Human melanoma cells transplanted into zebrafish proliferate, migrate, produce melanin, form masses and stimulate angiogenesis in zebrafish. Angiogenesis *9*, 139–151.

Huang, B., Lei, Z., Zhang, G.M., Li, D., Song, C., Li, B., Liu, Y., Yuan, Y., Unkeless, J., Xiong, H., and Feng, Z.H. (2008). SCF-mediated mast cell infiltration and activation exacerbate the inflammation and immunosuppression in tumor microenvironment. Blood *112*, 1269–1279.

Jung, D.W., Che, Z.M., Kim, J., Kim, K., Kim, K.Y., Williams, D., and Kim, J. (2010). Tumor-stromal crosstalk in invasion of oral squamous cell carcinoma: a pivotal role of CCL7. Int. J. Cancer *127*, 332–344.

Kalluri, R., and Zeisberg, M. (2006). Fibroblasts in cancer. Nat. Rev. Cancer *6*, 392–401.

Kamal, A., Thao, L., Sensintaffar, J., Zhang, L., Boehm, M.F., Fritz, L.C., and Burrows, F.J. (2003). A high-affinity conformation of Hsp90 confers tumour selectivity on Hsp90 inhibitors. Nature *425*, 407–410.

Kim, Y.K., and Chang, Y.T. (2007). Tagged library approach facilitates forward chemical genetics. Mol. Biosyst. *3*, 392–397.

Kolata, G. (2009, December 28). Old ideas spur new approaches in cancer fight. *The New York Times*.

Langley, R.R., and Fidler, I.J. (2011). The seed and soil hypothesis revisited—the role of tumor-stroma interactions in metastasis to different organs. Int. J. Cancer *128*, 2527–2535.

Li, Y., Zhang, T., Schwartz, S.J., and Sun, D. (2009). New developments in Hsp90 inhibitors as anti-cancer therapeutics: mechanisms, clinical perspective and more potential. Drug Resist. Updat. *12*, 17–27.

Liu, S., and Leach, S.D. (2011). Zebrafish models for cancer. Annu. Rev. Pathol. *6*, 71–93.

Marques, I.J., Weiss, F.U., Vlecken, D.H., Nitsche, C., Bakkers, J., Lagendijk, A.K., Partecke, L.I., Heidecke, C.D., Lerch, M.M., and Bagowski, C.P. (2009). Metastatic behaviour of primary human tumours in a zebrafish xenotransplantation model. BMC Cancer *9*, 128.

McCleese, J.K., Bear, M.D., Fossey, S.L., Mihalek, R.M., Foley, K.P., Ying, W., Barsoum, J., and London, C.A. (2009). The novel HSP90 inhibitor STA-1474 exhibits biologic activity against osteosarcoma cell lines. Int. J. Cancer *125*, 2792–2801.

Min, J., Kyung Kim, Y., Cipriani, P.G., Kang, M., Khersonsky, S.M., Walsh, D.P., Lee, J.Y., Niessen, S., Yates, J.R., 3rd, Gunsalus, K., et al. (2007).

Forward chemical genetic approach identifies new role for GAPDH in insulin signaling. Nat. Chem. Biol. *3*, 55–59.

Mosmann, T. (1983). Rapid colorimetric assay for cellular growth and survival: application to proliferation and cytotoxicity assays. J. Immunol. Methods *65*, 55–63.

Nakai, R., Ishida, H., Asai, A., Ogawa, H., Yamamoto, Y., Kawasaki, H., Akinaga, S., Mizukami, T., and Yamashita, Y. (2006). Telomerase inhibitors identified by a forward chemical genetics approach using a yeast strain with shortened telomere length. Chem. Biol. *13*, 183–190.

Orimo, A., Gupta, P.B., Sgroi, D.C., Arenzana-Seisdedos, F., Delaunay, T., Naeem, R., Carey, V.J., Richardson, A.L., and Weinberg, R.A. (2005). Stromal fibroblasts present in invasive human breast carcinomas promote tumor growth and angiogenesis through elevated SDF-1/CXCL12 secretion. Cell *121*, 335–348.

Pearl, L.H., and Prodromou, C. (2000). Structure and in vivo function of Hsp90. Curr. Opin. Struct. Biol. *10*, 46–51.

Proost, P., Struyf, S., Couvreur, M., Lenaerts, J.P., Conings, R., Menten, P., Verhaert, P., Wuyts, A., and Van Damme, J. (1998). Posttranslational modifications affect the activity of the human monocyte chemotactic proteins MCP-1 and MCP-2: identification of MCP-2(6-76) as a natural chemokine inhibitor. J. Immunol. *160*, 4034–4041.

Qing, G., Yan, P., Qu, Z., Liu, H., and Xiao, G. (2007). Hsp90 regulates processing of NF-kappa B2 p100 involving protection of NF-kappa B-inducing kinase (NIK) from autophagy-mediated degradation. Cell Res. *17*, 520–530.

Rouhi, P., Jensen, L.D., Cao, Z., Hosaka, K., Länne, T., Wahlberg, E., Steffensen, J.F., and Cao, Y. (2010). Hypoxia-induced metastasis model in embryonic zebrafish. Nat. Protoc. *5*, 1911–1918.

Saito, K., Oku, T., Ata, N., Miyashiro, H., Hattori, M., and Saiki, I. (1997). A modified and convenient method for assessing tumor cell invasion and migration and its application to screening for inhibitors. Biol. Pharm. Bull. *20*, 345–348.

Schreiber, S.L. (1998). Chemical genetics resulting from a passion for synthetic organic chemistry. Bioorg. Med. Chem. *6*, 1127–1152.

Schulte, T.W., and Neckers, L.M. (1998). The benzoquinone ansamycin 17-allylamino-17-demethoxygeldanamycin binds to HSP90 and shares important biologic activities with geldanamycin. Cancer Chemother. Pharmacol. *42*, 273–279.

Sharp, S.Y., Boxall, K., Rowlands, M., Prodromou, C., Roe, S.M., Maloney, A., Powers, M., Clarke, P.A., Box, G., Sanderson, S., et al. (2007). In vitro biological characterization of a novel, synthetic diaryl pyrazole resorcinol class of heat shock protein 90 inhibitors. Cancer Res. *67*, 2206–2216.

Solit, D.B., Ivy, S.P., Kopil, C., Sikorski, R., Morris, M.J., Slovin, S.F., Kelly, W.K., DeLaCruz, A., Curley, T., Heller, G., et al. (2007). Phase I trial of 17-allylamino-17-demethoxygeldanamycin in patients with advanced cancer. Clin. Cancer Res. *13*, 1775–1782.

Stern, H.M., and Zon, L.I. (2003). Cancer genetics and drug discovery in the zebrafish. Nat. Rev. Cancer *3*, 533–539.

Taylor, A.M., and Zon, L.I. (2009). Zebrafish tumor assays: the state of transplantation. Zebrafish *6*, 339–346.

Thompson, W.L., and Van Eldik, L.J. (2009). Inflammatory cytokines stimulate the chemokines CCL2/MCP-1 and CCL7/MCP-3 through NFkB and MAPK dependent pathways in rat astrocytes [corrected]. Brain Res. *1287*, 47–57.

Tropea, J.E., Cherry, S., and Waugh, D.S. (2009). Expression and purification of soluble His(6)-tagged TEV protease. Methods Mol. Biol. *498*, 297–307.

Vokes, E.E., Weichselbaum, R.R., Lippman, S.M., and Hong, W.K. (1993). Head and neck cancer. N. Engl. J. Med. *328*, 184–194.

Walter, S., and Buchner, J. (2002). Molecular chaperones—cellular machines for protein folding. Angew. Chem. Int. Ed. Engl. *41*, 1098–1113.

Wani, M.C., Taylor, H.L., Wall, M.E., Coggon, P., and McPhail, A.T. (1971). Plant antitumor agents. VI. The isolation and structure of taxol, a novel antileukemic and antitumor agent from Taxus brevifolia. J. Am. Chem. Soc. *93*, 2325–2327.

West, M.A., Billiar, T.R., Curran, R.D., Hyland, B.J., and Simmons, R.L. (1989). Evidence that rat Kupffer cells stimulate and inhibit hepatocyte protein synthesis in vitro by different mechanisms. Gastroenterology *96*, 1572–1582.

Williams, D., Jung, D.W., Khersonsky, S.M., Heidary, N., Chang, Y.T., and Orlow, S.J. (2004). Identification of compounds that bind mitochondrial F1F0 ATPase by screening a triazine library for correction of albinism. Chem. Biol. *11*, 1251–1259.

Williams, D.R., Ko, S.K., Park, S., Lee, M.R., and Shin, I. (2008). An apoptosis-inducing small molecule that binds to heat shock protein 70. Angew. Chem. Int. Ed. Engl. *47*, 7466–7469.

Witz, I.P. (2008). Tumor-microenvironment interactions: dangerous liaisons. Adv. Cancer Res. *100*, 203–229.

Youngs, S.J., Ali, S.A., Taub, D.D., and Rees, R.C. (1997). Chemokines induce migrational responses in human breast carcinoma cell lines. Int. J. Cancer *71*, 257–266.

